

Research Article

Seismic Response for Wave Propagation across Joints with Equally and Unequally Close-Open Behaviours

Qi Zhang ^{1,2}, Zhengliang Li ¹ and Tao Yu¹

¹School of Civil Engineering, Southeast University, Nanjing 210096, China

²State Key Laboratory for GeoMechanics and Deep Underground Engineering, China University of Mining & Technology, Xuzhou 221116, China

Correspondence should be addressed to Zhengliang Li; lzlyy92@163.com

Received 10 May 2018; Revised 3 September 2018; Accepted 18 September 2018; Published 16 October 2018

Guest Editor: Qianbing Zhang

Copyright © 2018 Qi Zhang et al. This is an open access article distributed under the Creative Commons Attribution License, which permits unrestricted use, distribution, and reproduction in any medium, provided the original work is properly cited.

The interaction between rock joints and seismic waves is critical in rock engineering when rock mass is suffered from human-induced or natural earthquakes. Stress wave propagation across rock joints is usually dependent on the seismic response of the joints. Wave propagation may cause joints close or open under the in situ stress. In this paper, the seismic response for wave propagation with an arbitrary incident angle impinging on joints is studied. Both reflection and transmission usually occurring at the two interfaces of the joint are considered, respectively. Wave propagation equations with equally and unequally close-open behaviours are deduced firstly, which can be applied for the general cases of arbitrary incident P- or S-wave. Then, wave propagation across joints with normal and oblique incident P- and S-waves is analyzed by considering the equally and unequally close-open behaviours and verified by comparing with the existing methods. Finally, several parametric studies are conducted to evaluate the effect of in situ stress on transmitted waves, the effect of the incident frequency on the maximum deformation of joints, and the effect of the incident angle on the maximum deformation of joints. The wave propagation equations derived in the study are more feasible and can well analyze the seismic response of wave propagation for the most general cases of different incident waveforms.

1. Introduction

The safety and stability of underground engineering are often affected by seismic waves, which may come from human-induced or natural earthquakes. Since the underground engineering is surrounded by jointed rock mass, the rock joints not only govern the mechanical behavior of the rock mass but also influence wave propagation in the rock mass. Study on the interaction between stress wave and rock joints is critical to evaluate the stability and safety of underground engineering under seismic loads.

The natural rock joints are generally nonwelded. The two sides of a joint may have relative deformation, such as opening, closure, and slip under normal and shear stresses during seismic wave propagation [1–3]. When a rock joint is not able to sustain tensile stresses, the joint is open and then its two sides become free surfaces to reflect seismic waves

impinging on the joint. The mechanical behavior of a joint is a main factor to affect stress wave propagation across jointed rock mass. Bandis et al. [4] observed that the normal property of a rock joint appears nonlinear elastic and its pressure-closure relation is like a hyperbolic curve.

For the normal cases, the displacement discontinuity method (DDM) was applied commonly for wave propagation across rock joints [5, 6]. Zhao et al. [7] and Zhao et al. [8] developed a method coupling DDM to derive a wave propagation equation across linear and nonlinear joints, respectively. Zhu et al. [9] improved the DDM to analyze the effect of viscoelastic behavior of filled joints on seismic wave propagation. Li et al. [10] and Li [11] proposed a time domain recursive method coupled with the DDM to analyze the wave propagation across the parallel joints with linear or nonlinear property. In these studies, the close and open mechanical properties of a joint were considered to be the

same, and the stress-closure relation of joints was also adopted to describe the equally close-open behavior. Later, Li et al. [12] deduced an equation for wave propagation normally across joints with unequally close-open behavior based on the method of characteristic. The analysis result showed that the unequally close-open behavior of a joint as well as the in situ stress influences the wave attenuation.

For oblique cases, Kolsky [13] and Johnson [14] firstly conducted the studies of the interaction between an obliquely incident wave and a welded interface of two media, and established the relation (i.e., Snell's law) between the propagation speeds and the incident, transmitted, and reflected angles. Based on the DDM and Snell's law, the reflection and transmission coefficients for harmonic plane waves with an arbitrary incident angle impinging upon a plane linear slip interface were derived [6]. Close-form solutions in a matrix form normally impinging on a linear joint were obtained subsequently [15–17]. Li et al. [18] proposed a wave propagation equation for the interaction between obliquely incident P- or S-wave and a linear elastic rock joint. The study can be straightforwardly extended for different incident waveforms and nonlinear rock joints.

The study is motivated by the need to better understand the effect of an arbitrary incident angle on wave propagation and the seismic response of the joints with equally and unequally close-open behaviours. Wave propagation equations with an arbitrary incident angle are deduced for two deformation modes, i.e., close mode and open mode, respectively. Then wave propagation across joints for normal and oblique incident P- and S-waves is analyzed and verified with the equally and unequally close-open behaviours. Finally, parametric studies are conducted to evaluate the effect of in situ stress on transmitted waves, the effects of the incident frequency, and the incident angle on the maximum deformation of joints. It provides a theoretical background of seismic wave normally and obliquely interacting with a rock joint with equally and unequally close-open behaviours systemically.

2. Theoretical Formulations

2.1. Problem Description. Assume there is a joint in a linearly elastic, homogeneous, and isotropic rock. When a plane P- or S-wave impinges on one interface of the joint, both reflection and transmission usually occur at the two interfaces of the joint, as shown in Figure 1. In the most general case ($0 < \alpha \leq \alpha_c$ and $0 < \beta \leq \beta_c$), the incident, transmitted, and reflected waves satisfy Snell's law, where α and β are the emergence angles of the incident P- and S-waves, respectively. α_c and β_c are the critical angles of the incident P- and S-waves, respectively. During wave propagation, the joint may close or open. During the close process, the two interfaces begin to contact and interact, as shown in Figure 1(a). This interaction is dependent on the close behavior of the joint. When the joint is open, the two interfaces are separated from each other and become two free surfaces. The incident wave will be totally reflected from the joint, as shown in Figure 1(b). This study is to

analyze wave propagation across a joint with unequally close-open behaviors.

2.2. Wave Propagation Equations. Plane wave propagation across a joint is schematically shown in Figure 1. The interaction between the stress waves and the interfaces can be obtained from the derivation by Li and Ma [19]. If the in situ stress is considered, the expressions for the normal and tangential stresses σ^- and τ^- on the left interface are

$$\sigma^- = z_p \cos 2\beta v_{rp}^- + z_s \sin 2\beta v_{rs}^- + z_p \cos 2\beta v_{lp}^- \quad (1)$$

$$- z_s \sin 2\beta v_{ls}^- + \sigma_0,$$

$$\tau^- = \frac{z_p \sin 2\beta \tan \beta v_{rp}^-}{\tan \alpha} - z_s \cos 2\beta v_{rs}^- - \frac{z_p \sin 2\beta \tan \beta v_{lp}^-}{\tan \alpha} - z_s \cos 2\beta v_{ls}^-, \quad (2)$$

and the normal and tangential stresses σ^+ and τ^+ on the right interface are

$$\sigma^+ = z_p \cos 2\beta v_{rp}^+ + z_s \sin 2\beta v_{rs}^+ + \sigma_0, \quad (3)$$

$$\tau^+ = \frac{z_p \sin 2\beta \tan \beta v_{rp}^+}{\tan \alpha} - z_s \cos 2\beta v_{rs}^+, \quad (4)$$

where σ_0 is the in situ stress; z_p and z_s denote the wave impedance of P- and S-waves, and equal to the product of the density of the medium and the wave propagation velocity; v_{rp}^m and v_{lp}^m ($m = -, +$) are the particle velocities of right- and left-running P-waves on the two sides of the joint; and v_{rs}^m and v_{ls}^m ($m = -, +$) are the particle velocities of right- and left-running S-waves on the two sides of the joint.

The normal and tangential components, v_n^- and v_τ^- , of the velocity before the joint are

$$v_n^- = \cos \alpha v_{rp}^- + \sin \beta v_{rs}^- - \cos \alpha v_{lp}^- + \sin \beta v_{ls}^-, \quad (5)$$

$$v_\tau^- = \sin \alpha v_{rp}^- - \cos \beta v_{rs}^- + \sin \alpha v_{lp}^- + \cos \beta v_{ls}^-, \quad (6)$$

and the normal and tangential components, v_n^+ and v_τ^+ , of the velocity after the joint are

$$v_n^+ = \cos \alpha v_{rp}^+ + \sin \beta v_{rs}^+, \quad (7)$$

$$v_\tau^+ = \sin \alpha v_{rp}^+ - \cos \beta v_{rs}^+. \quad (8)$$

The relatively normal and tangential displacements of the joint, Δu_n and Δu_τ , are expressed as

$$\begin{aligned} u_n^- - u_n^+ &= \Delta u_n, \\ u_\tau^- - u_\tau^+ &= \Delta u_\tau. \end{aligned} \quad (9)$$

The initial closure of a joint is denoted as Δu_0 under the effect of in situ stress σ_0 . It is noted that the positive normal displacements u_n^m ($m = -, +$) refer to the right direction, and the positive tangential displacements u_τ^m ($m = -, +$) refer to the upward direction.

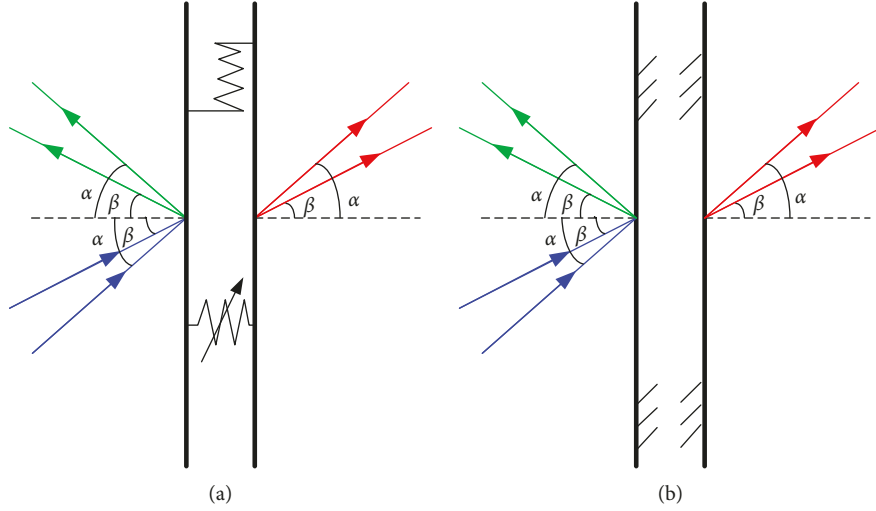


FIGURE 1: Schematic view for joint close-open process during wave propagation. (a) A closed joint. (b) An open joint.

During wave propagation, there are two possible deformation modes, i.e., close mode when $\Delta u_n \geq -\Delta u_0$ and open mode when $\Delta u_n < -\Delta u_0$.

- (1) Close mode when $\Delta u_n \geq -\Delta u_0$. When the joint is closed, both normal and tangential deformations of the joint are elastic and the joint becomes a displacement discontinuity boundary. For this case, the displacement discontinuity method (DDM) [5, 6] is adopted in the paper. In the DDM, the stresses before and after the joint are assumed to be continuous while the particle velocities before and after the joint are not continuous. Hence, the stresses on the two sides of the joint are

$$\begin{aligned} \sigma^- &= \sigma^+ = \sigma, \\ \tau^- &= \tau^+ = \tau, \end{aligned} \quad (10)$$

where σ is the normal stress on the joint sides. If the normal and shear properties of the joint satisfy the BB model [1, 4] and are linearly elastic, the relative normal and tangential displacements of the joint will satisfy

$$\begin{aligned} \Delta u_n &= \frac{\sigma}{(k_{ni} + \sigma/d_{\max})}, \\ \Delta u_\tau &= \frac{\tau}{k_s}, \end{aligned} \quad (11)$$

where k_{ni} is the initial normal stiffness and d_{\max} is the maximum allowable normal closure of the joint. Define $\bar{k}_n = (k_{ni} + (\sigma_i/d_{\max}))^2/k_{ni}$. When Equation (9) is differentiated with respect to time t , respectively, there are

$$\begin{cases} v_{n(i)}^- - v_{n(i)}^+ = \frac{1}{\bar{k}_n} \frac{\sigma_{i+1} - \sigma_i}{\Delta t}, \\ v_{\tau(i)}^- - v_{\tau(i)}^+ = \frac{1}{k_s} \frac{\partial \tau}{\partial t} = \frac{1}{k_s} \frac{\tau_{i+1} - \tau_i}{\Delta t}, \end{cases} \quad (12)$$

where Δt is a small-time interval. When Equations (1) to (8) are combined with Equations (10) and (12), the reflected and transmitted waves can be derived and expressed in a matrix form.

$$\begin{bmatrix} v_{lp}^- \\ v_{rs}^- \end{bmatrix}_i = -B^{-1}A \begin{bmatrix} v_{rp}^- \\ v_{rs}^- \end{bmatrix}_i + B^{-1}A \begin{bmatrix} v_{rp}^+ \\ v_{rs}^+ \end{bmatrix}_i, \quad (13)$$

$$\begin{bmatrix} v_{rp}^+ \\ v_{rs}^+ \end{bmatrix}_{i+1} = A^{-1}C \begin{bmatrix} v_{rp}^+ \\ v_{rs}^+ \end{bmatrix}_i + A^{-1}D \begin{bmatrix} v_{rp}^- \\ v_{rs}^- \end{bmatrix}_i + A^{-1}E \begin{bmatrix} v_{lp}^- \\ v_{ls}^- \end{bmatrix}_i, \quad (14)$$

where matrix parameters A to E are written as

$$A = \begin{bmatrix} z_p \cos 2\beta & z_s \sin 2\beta \\ \frac{z_p \sin 2\beta \tan \beta}{\tan \alpha} & -z_s \cos 2\beta \end{bmatrix}, \quad (15)$$

$$B = \begin{bmatrix} z_p \cos 2\beta & -z_s \sin 2\beta \\ -\frac{z_p \sin 2\beta \tan \beta}{\tan \alpha} & -z_s \cos 2\beta \end{bmatrix}, \quad (16)$$

$$C = \begin{bmatrix} z_p \cos 2\beta - \bar{k}_n \Delta t \cos \alpha & z_s \sin 2\beta - \bar{k}_n \Delta t \sin \beta \\ \frac{z_p \sin 2\beta \tan \beta}{\tan \alpha} - k_s \Delta t \sin \alpha & -z_s \cos 2\beta + k_s \Delta t \cos \beta \end{bmatrix}, \quad (17)$$

$$D = \begin{bmatrix} \bar{k}_n \Delta t \cos \alpha & \bar{k}_n \Delta t \sin \beta \\ k_s \Delta t \sin \alpha & -k_s \Delta t \cos \beta \end{bmatrix}, \quad (18)$$

$$E = \begin{bmatrix} -\bar{k}_n \Delta t \cos \alpha & \bar{k}_n \Delta t \sin \beta \\ k_s \Delta t \sin \alpha & k_s \Delta t \cos \beta \end{bmatrix}. \quad (19)$$

Equations (13) and (14) and the expressions of A to E shown in Equations (15) to (19) are consistent with the wave propagation equation derived by Li [11] when the joint is in the elastic mode without relative slip.

(2) Open mode when $\Delta u_n < -\Delta u_0$. When the joint is open, the normal and tangential deformations of the joint are not elastic any more, and the two interfaces of the joint become the two free surfaces.

$$\begin{aligned} \sigma^- &= \sigma^+ = 0, \\ \tau^- &= \tau^+ = 0. \end{aligned} \quad (20)$$

From Equations (1) and (2), we get

$$\begin{bmatrix} v_{lp}^- \\ v_{ls}^- \end{bmatrix}_i = -B^{-1} A \begin{bmatrix} v_{lp}^- \\ v_{rs}^- \end{bmatrix}_i - B^{-1} \begin{bmatrix} \sigma_0 \\ 0 \end{bmatrix}, \quad (21)$$

and from Equations (3) and (4), we get

$$\begin{bmatrix} v_{lp}^+ \\ v_{rs}^+ \end{bmatrix}_i = -A^{-1} \begin{bmatrix} \sigma_0 \\ 0 \end{bmatrix}, \quad (22)$$

where the matrix parameters A and B are expressed in Equations (15) and (16).

3. Wave Propagation across Joints with Equally and Unequally Close-Open Behaviours

In this section, incident P- and S-waves with an arbitrary incident angle impinge on two types of joints: joints with the equally close-open behaviors and joints with unequally close-open behaviors. The in situ stresses σ_0 are assumed to be 0 and $0.5z_p A_i$, respectively. The incident wave is assumed as a one-cycle sinusoidal waveform, i.e.,

$$v_I = \begin{cases} A_i \sin(\omega t), & t = 0 \sim \frac{1}{f_0}, \\ 0, & t > \frac{1}{f_0}, \end{cases} \quad (23)$$

where $\omega = 2\pi f_0$, $f_0 = 50$ Hz. A_i is assumed to be 0.1 m/s, which is the amplitude of the incident waves.

Some basic parameters for the joint and the adjacent rocks are as follows. The maximum allowable normal closure

d_{\max} is 1 mm, and the initial normal stiffness k_{ni} is 1.0 GPa/m. The shear stiffness k_s equals k_{ni} , and the rock mass density ρ is 2650 kg/m³. The P-wave velocity c_p is 5840 m/s, and the shear wave velocity c_s is 2950 m/s.

3.1. Normal Case. When an incident P-wave with the form of Equation (23) impinges normally on one side of the joint, the transmitted and reflected waves with the equally close-open behavior can be calculated from Equations (13) and (14). The calculation results are shown in Figures 2(a) and 2(b) for in situ stresses σ_0 being 0 and $0.5z_p A_i$, respectively. It can be observed from Figures 2(a) and 2(b) that either the maximum or the minimum value of the transmitted wave for $\sigma_0 = 0.5z_p A_i$ is obviously greater than that for $\sigma_0 = 0$. For the same incident P-wave, when the close-open behaviors of the joint are unequal, Figures 2(c) and 2(d) show the transmitted and reflected waves following Equations (13) and (14) during the joint close process and Equations (21) and (22) during the joint open process. These two figures also show that the in situ stress can result in the increasing peak values of the transmitted wave. Meanwhile, by comparing the Figures 2(a) and 2(b), it can be found that the tensile portion of the transmitted wave for no in situ stress or $\sigma_0 = 0$ is completely cut off and the tensile portion of the transmitted wave for $\sigma_0 = 0.5z_p A_i$ is partly cut off. The cut-off value of the transmitted wave is related to the in situ stress. In other words, the tensile portion of the transmitted wave is cut off if its particle velocity is less than $-\sigma_0/z_p$.

The particle velocities for the two sides of the joint can be calculated from Equations (5) to (8) when the transmitted and reflected waves are obtained. The relative normal and tangential displacements of the joint are then calculated from Equation (9) when the particle velocities for the two joint sides are integrated to time t . Figures 3(a) and 3(b) show the normal displacements according to the transmitted and reflected waves shown in Figure 1, where Figures 3(a) and 3(b) are for the joints with the equally and unequally close-open behaviors, respectively. Comparison between Figures 3(a) and 3(b) show that for $\sigma_0 = 0$, the joint closes firstly, then opens gradually, and finally keeps around 1 mm in open displacement when the joint has the unequally close-open behavior. For the equally close-open behavior, the joint closes firstly, then gradually opens and finally closes.

3.2. Oblique Case. If the incident P-wave with the form of Equation (23) obliquely impinges on one side of the joint, wave propagation can also be calculated from Equations (13) and (14) and Equations (21) and (22). Figures 4(a) and 4(b) show the transmitted and reflected waves when the incident angle is 20° and the in situ stress is $0.5z_p A_i$, where Figure 4(a) is for the joint with the equally close-open behavior while Figure 4(b) is for the joint with unequally close-open behavior. Comparison indicates that the compressive portions of the transmitted P-waves shown in Figures 4(a) and 4(b) are identical, while the tensile portion of the transmitted P-wave shown in Figure 4(b) is cut off when the particle velocity is less than -0.05 m/s. When the joint is open and two interfaces are not

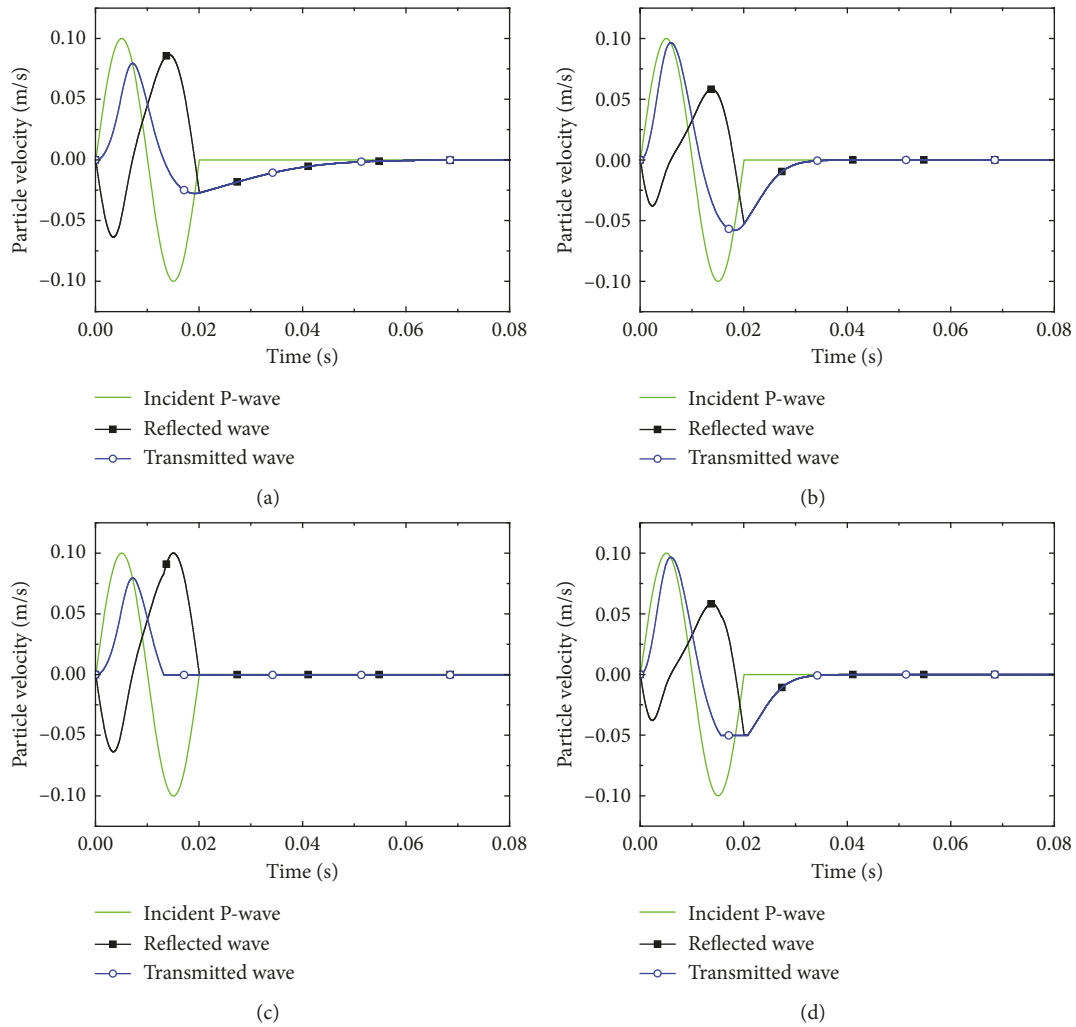


FIGURE 2: Wave propagation normally across a joint with equally and unequally close-open behaviours ($f = 50$ Hz). Joint with equally close-open behaviour (a) $\sigma_0 = 0$ and (b) $\sigma_0 = 0.5z_p A_i$. Joint with unequally close-open behaviour (c) $\sigma_0 = 0$ and (d) $\sigma_0 = 0.5z_p A_i$.

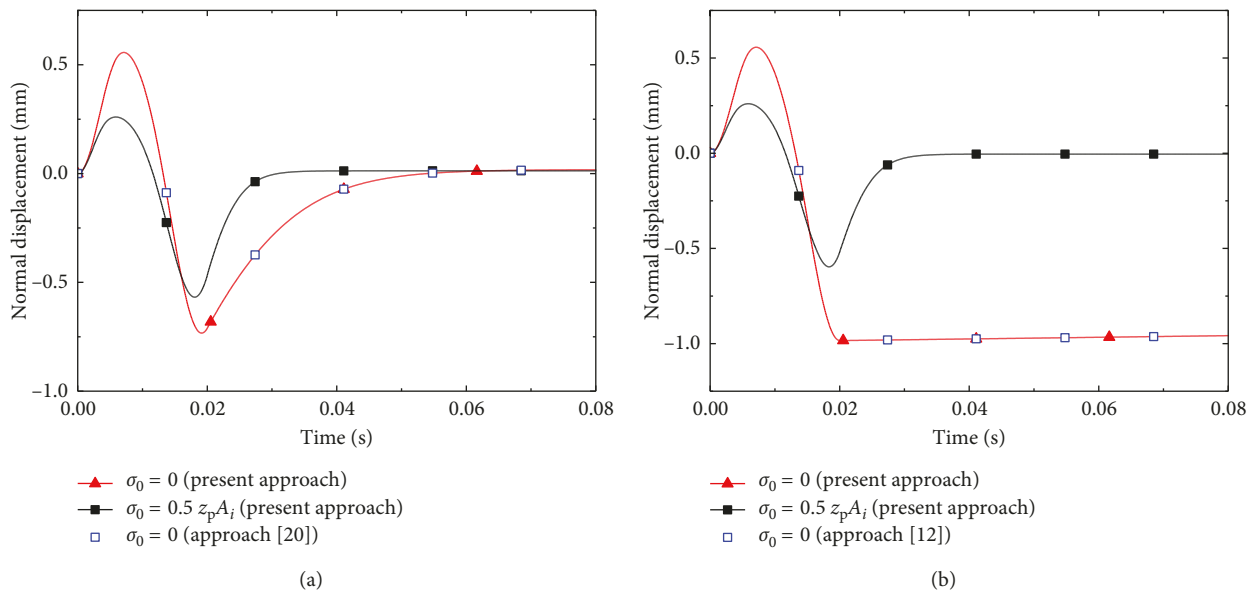


FIGURE 3: Joint closure during wave propagation normally ($f = 50$ Hz). (a) Joint with equally close-open behaviour. (b) Joint with unequally close-open behaviour.

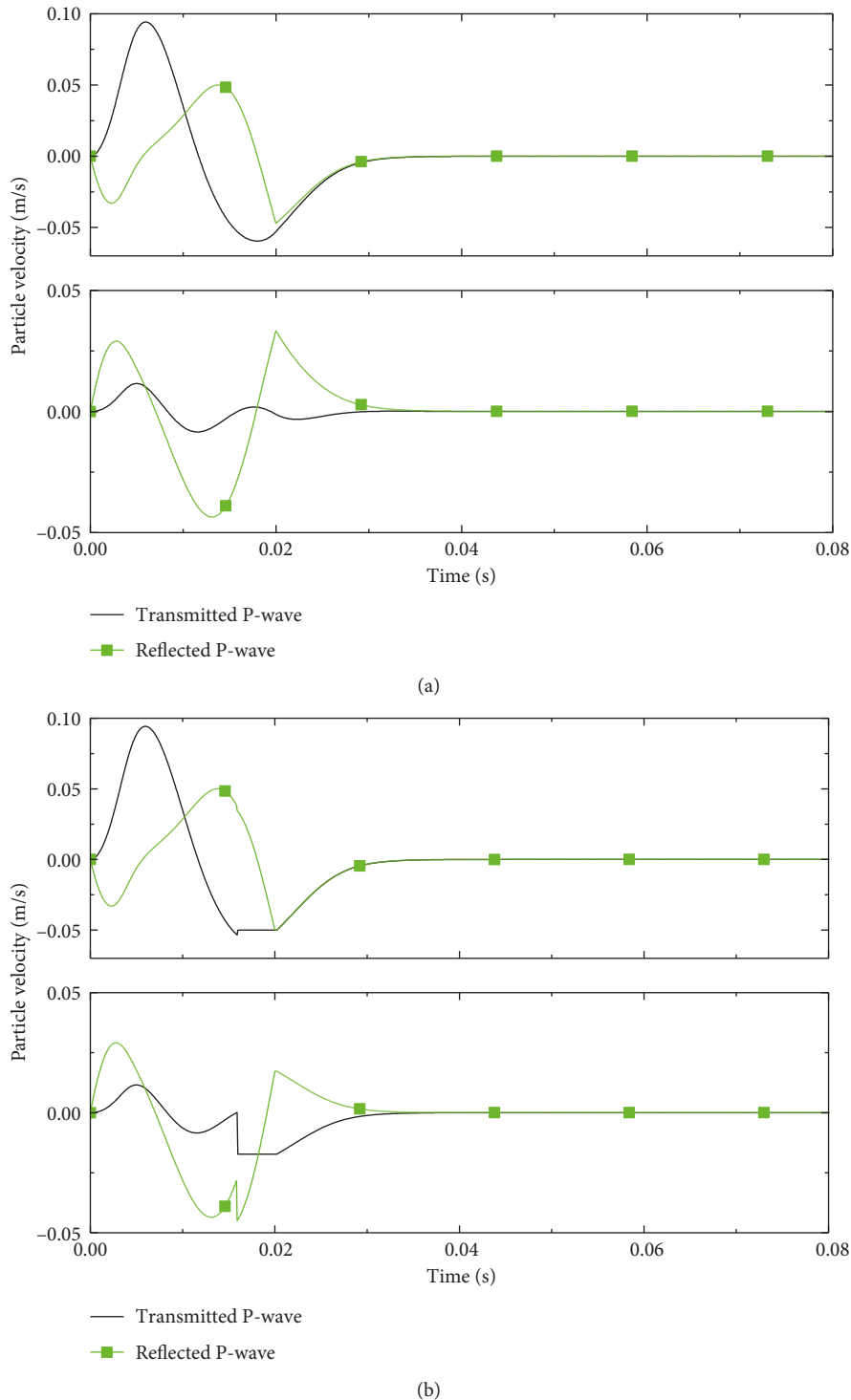


FIGURE 4: Wave propagation obliquely across a joint with equally and unequally close-open behaviour ($\alpha = 20^\circ$, $\sigma_0 = 0.5z_p A_i$, $f = 50$ Hz). (a) Joint with equally close-open behaviour. (b) Joint with unequally close-open behaviour.

interacted, the shear strength of the joint becomes zero and the relative slip of the joint occurs simultaneously. Therefore, the partly cut-off of the transmitted P-wave corresponds to the relative slip of the joint, which can be observed from the transmitted S-wave shown in Figure 4 (b). When the joint is open, the two interfaces are

interacted in elastic behavior. The normal and tangential deformations of the joint are elastic and no relative slip occurs, as shown in Figure 4(a).

With the transmitted and reflected waves shown in Figure 4, the normal and tangential relative displacements of the joint can be calculated as shown in Figure 5, which

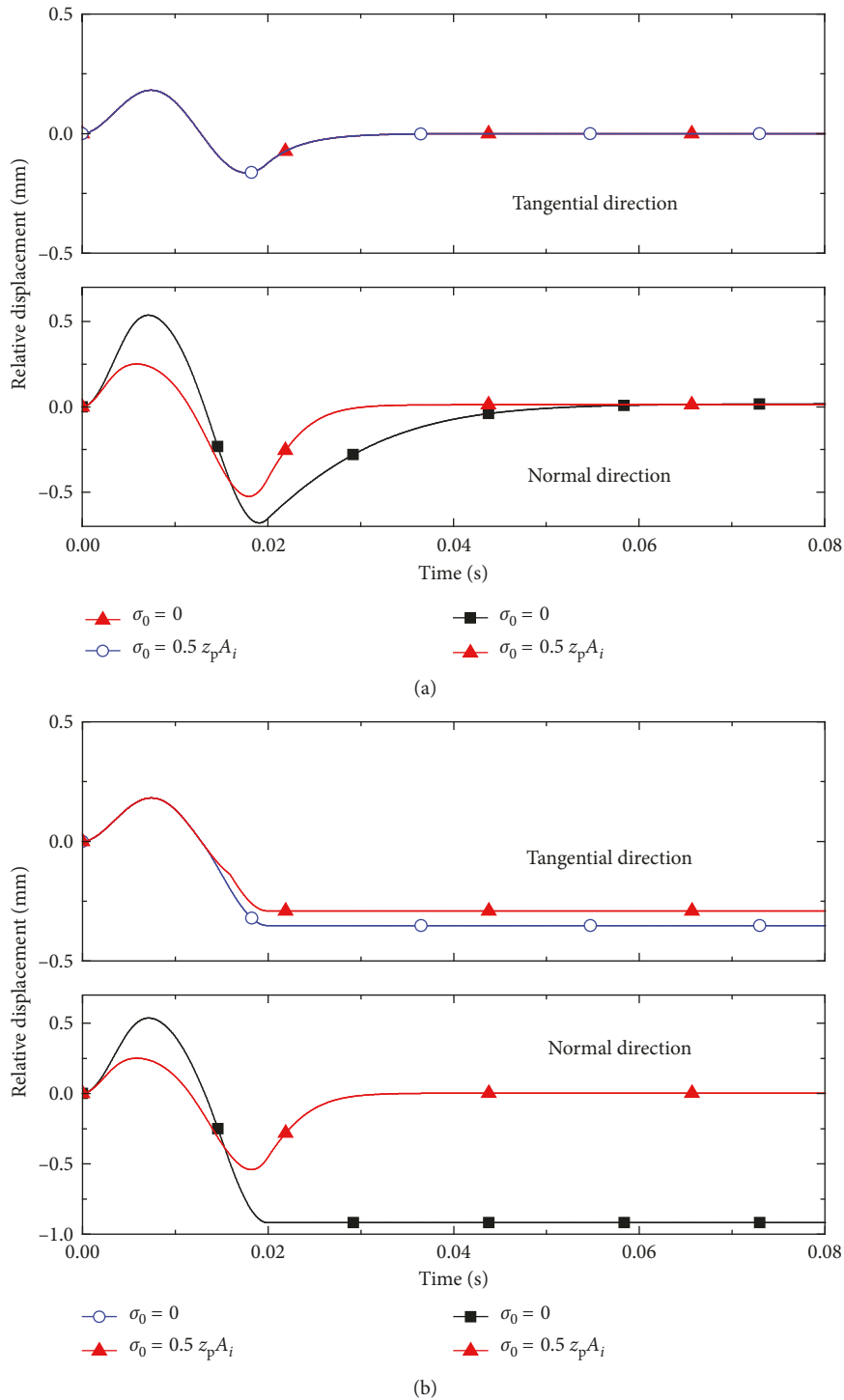


FIGURE 5: Normal and tangential relative displacement of the joint during wave propagation obliquely ($f = 50 \text{ Hz}$, $\alpha = 20^\circ$). (a) Without considering open property of joints. (b) With considering open property of joints.

also shows the results when the in situ stress is zero. Figures 5(a) and 5(b) are for the joints with the equally and unequally close-open behaviors, respectively. Compared with Figure 5(a), Figure 5(b) shows that the relative slip of the joint occurs for two in situ stresses, i.e., $\sigma_0 = 0$ and $\sigma_0 = 0.5z_pA_i$. The value of the relative slip of the joint for $\sigma_0 = 0$ is bigger than that of $\sigma_0 = 0.5z_pA_i$, which indicates that lower

in situ stress easily causes joint open and the slippery deformation of the joint.

3.3. *Verification with Existing Methods.* Based on the characteristic line theory and DDM, Zhao and Cai [20] derived the wave propagation equation for incident P-waves across a single nonlinear rock joint with equally

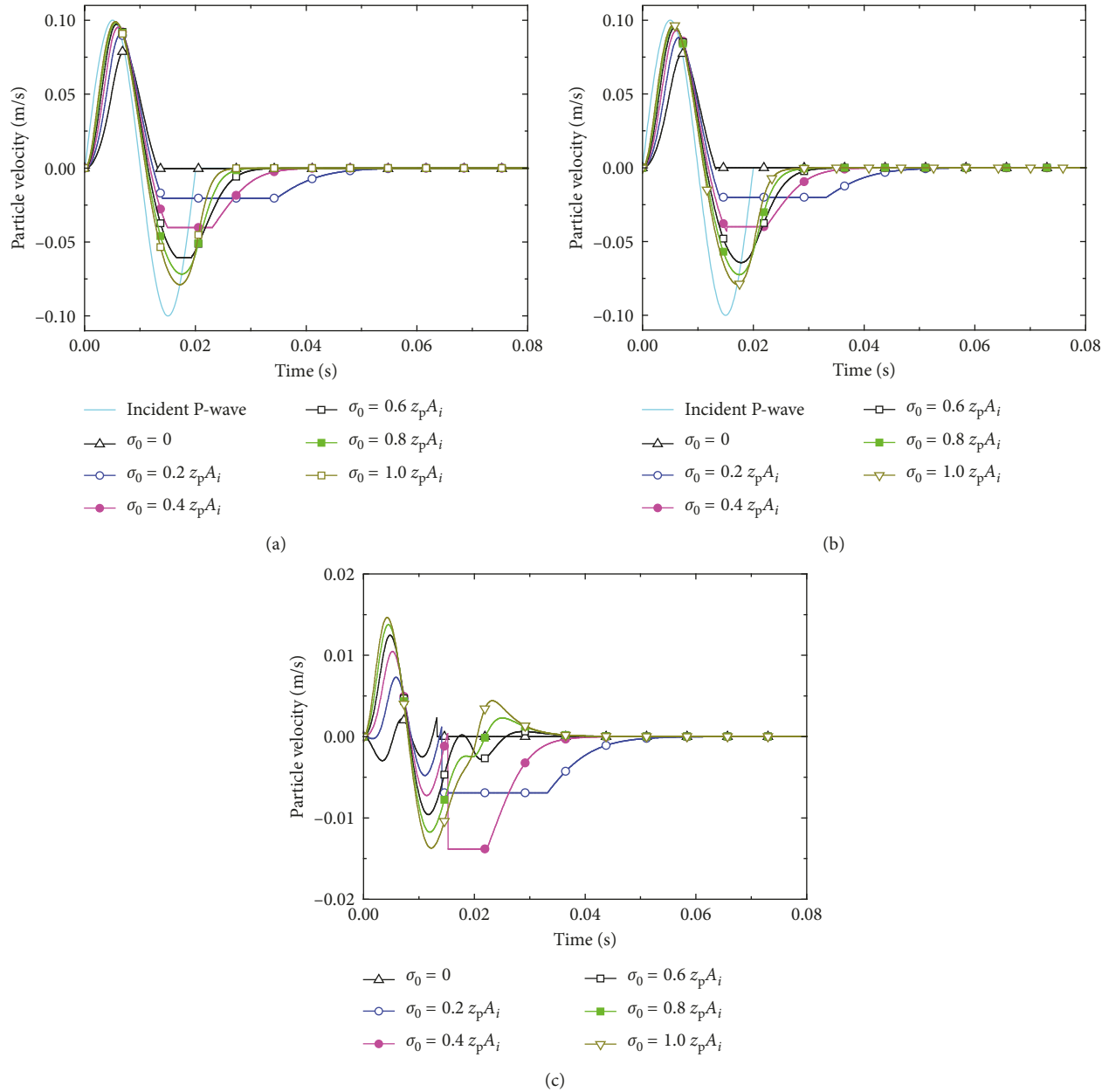


FIGURE 6: Transmitted P- and S-waves for incident P-wave propagation across joint with unequally close-open behaviour ($f = 50$ Hz). (a) Normal case, incident P-wave, and transmitted P-waves. (b) $\alpha = 20^\circ$, incident P-wave, and transmitted P-waves. (c) $\alpha = 20^\circ$, incident P-wave, and transmitted S-waves.

close-open behavior. Li et al. [12] employed characteristic line theory and DDM to analyze the interaction between stress waves and rock joints with unequally close-open behavior. The results are plotted as the scattered points in Figures 3(a) and 3(b), for incident P-waves normally impinging on nonlinear rock joints with equally and unequally close-open behaviors, respectively. By comparison, it is observed that the results from the present approach agree with those obtained by Zhao and Cai [20] and Li et al. [12], which indicates that wave propagation equations proposed in Section 2.2 can well reflect the seismic response of joints with equally and unequally close-open behaviors during wave propagation.

4. Parametric Studies

This section is to carry out parametric studies to analyze wave propagation and the seismic response of joints when the incident P- and S-waves with the form of Equation (23) normally and obliquely impinge on a joint. During the closing process, the joint is assumed to have the normal property with BB model and the tangential property with linearly elastic. Once the joint is open, the two interfaces of the joint are not interacted. Equations (13), (14), (21), and (22) are adopted to calculate the transmitted wave. The parameters of the joint and the incident waves shown in Section 3 will be adopted.

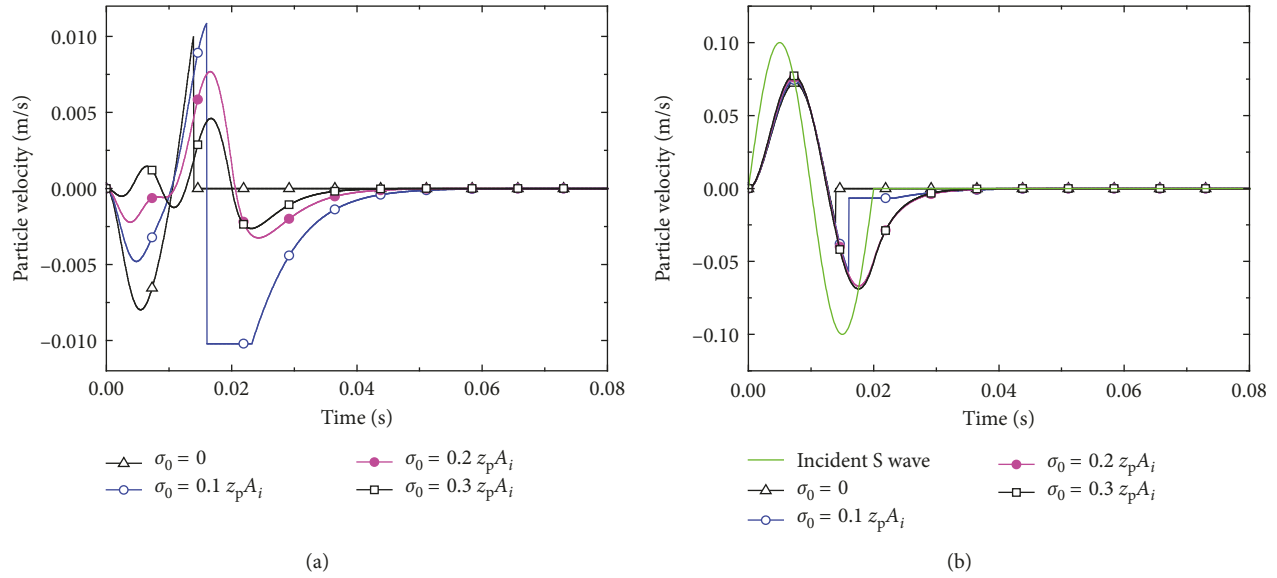


FIGURE 7: Transmitted P- and S-waves for incident S-wave propagation across joint with unequally close-open behaviour ($f = 50$ Hz). (a) $\beta = 20^\circ$, incident S-wave, and transmitted P-waves. (b) $\beta = 20^\circ$, incident S-wave, and transmitted S-waves.

4.1. Effect of In Situ Stress on Transmitted Waves.

Figures 6 and 7 show the transmitted waves when incident P- and S-waves normally and obliquely impinge on the joint, respectively, where the in situ stress σ_0 changes from zero to $1.0z_p A_i$. It can be seen from Figures 6(a) and 6(b) that when the in situ stress is small, such as $\sigma_0 = 0 \sim 0.6z_p A_i$ for a normal incidence or $\sigma_0 = 0 \sim 0.4z_p A_i$ for an oblique incident P-wave with an incident angle $\alpha = 20^\circ$, the opening deformation of the joint occurs. During the opening process, the particle velocity of the transmitted P-wave equals σ_0/z_p and the relative slip occurs simultaneously. The duration of the relative slip decreases with the increasing in situ stress. For the oblique case, during the slippery process of the joint, the particle velocity of the joint caused by the transmitted S-wave (i.e., the slippery velocity of the right side of the joint) increases with the increasing in situ stress.

When an incident S-wave impinges on the joint with an incident angle $\beta = 20^\circ$, the transmitted P- and S-waves are calculated and shown in Figure 7 when the in situ stress varies from zero to $0.3z_p A_i$. Although we assume that the shear property of the joint is linearly elastic, the relative slip deformation still occurs for the joint when the in situ stress is zero or $0.1z_p A_i$, as shown in Figure 7. The reason to cause the slip deformation is the opening of the joint during the wave propagation. When an incident S-wave impinges on the joint, four waves (i.e., reflected and transmitted P- and S-waves) are produced from the joint interfaces. When the tensile stress acted on the two interfaces of the joint is bigger than the in situ stress, the joint is open and its shear strength falls to zero, and then the relative slip of the joint occurs.

Figures 8(a) and 8(b) show the amplitude spectra of the transmitted P-waves shown in Figures 6(a) and 6(b), respectively. It can be found that the dominant frequencies of the transmitted P-waves are around 35.6 Hz for the normal case and 33.4 or 40 Hz for the oblique case, when the joint

is always closed during wave propagation. Comparatively speaking, when the open mode takes place, the corresponding dominant frequency of the transmitted P-wave will drop. It also can be found that the smaller in situ stress is related to the lower dominant frequency of the transmitted P-wave. For example, when σ_0 is $0.2z_p A_i$, the dominant frequencies are 21.4 Hz and 20.1 Hz for the normal and oblique cases. When σ_0 is $0.4z_p A_i$, the dominant frequencies are 28.5 Hz and 26.8 Hz for normal and oblique cases. It has been calculated by [7] that the dominant frequency is 42.5 Hz for the incident wave with the waveform of Equation (23). The amplitude spectra shown in Figure 8 indicate that the joint filters out high frequency waves, especially when the joint is open during wave propagation.

4.2. Effect of Incident Frequency on the Maximum Deformation of Joints.

In this section, the effect of the incident P-wave's frequency on the maximum opening deformation and slip of the joint is studied when the incident angle α is 20° . Equations (13), (14), (21), and (22) are used to calculate the reflected and transmitted waves and Equations (5)–(9) are adopted to calculate the relative normal and tangential displacements of the joint. Figures 9(a) and 9(b) show the relationship between the frequency of the incident P-wave and the maximum opening deformation and the maximum slip of the joint, respectively, when the in situ stress varies from zero to $0.8z_p A_i$. The two figures show that both the maximum opening deformation and the maximum slip of the joint monotonously decrease with the increasing incident frequency. The maximum opening deformation and slip decrease sharply for the lower frequency, and then decrease slowly for the higher frequency. It is shown in Figure 9(a) that for a given frequency, the maximum opening deformation for $\sigma_0 = 0$ is the largest, while the maximum opening for σ_0 equal to $0.8z_p A_i$ is the

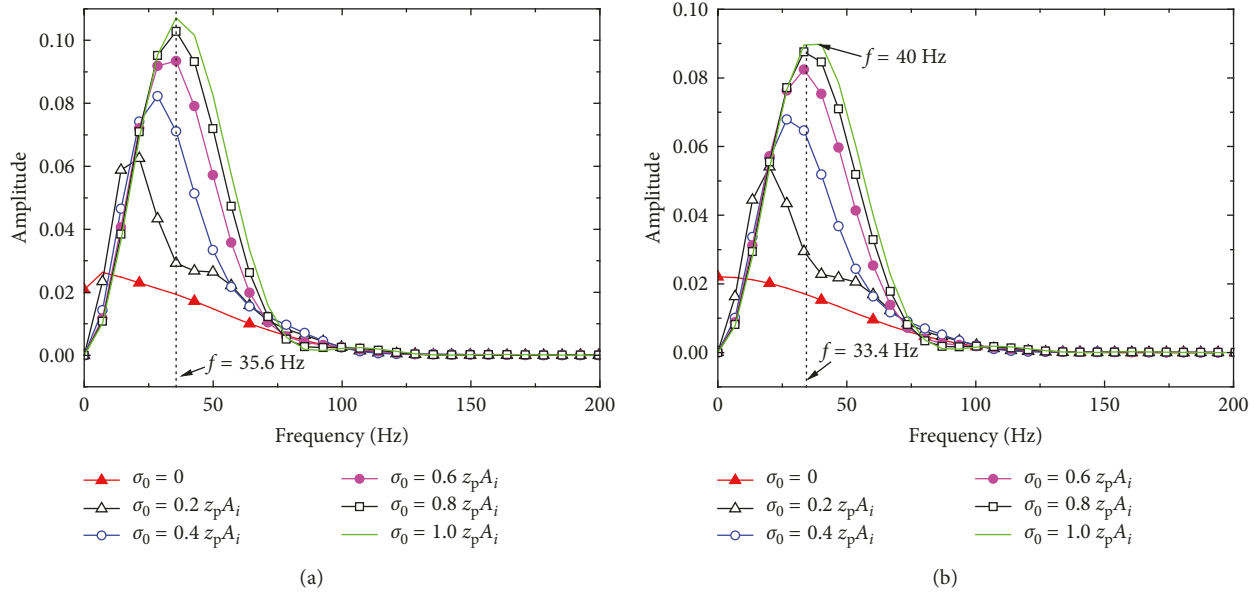


FIGURE 8: Amplitude spectra of the transmitted P-waves shown in Figures 6(a) and 6(b) ($f = 50$ Hz, $\alpha = 20^\circ$). (a) Normal case. (b) Oblique case.

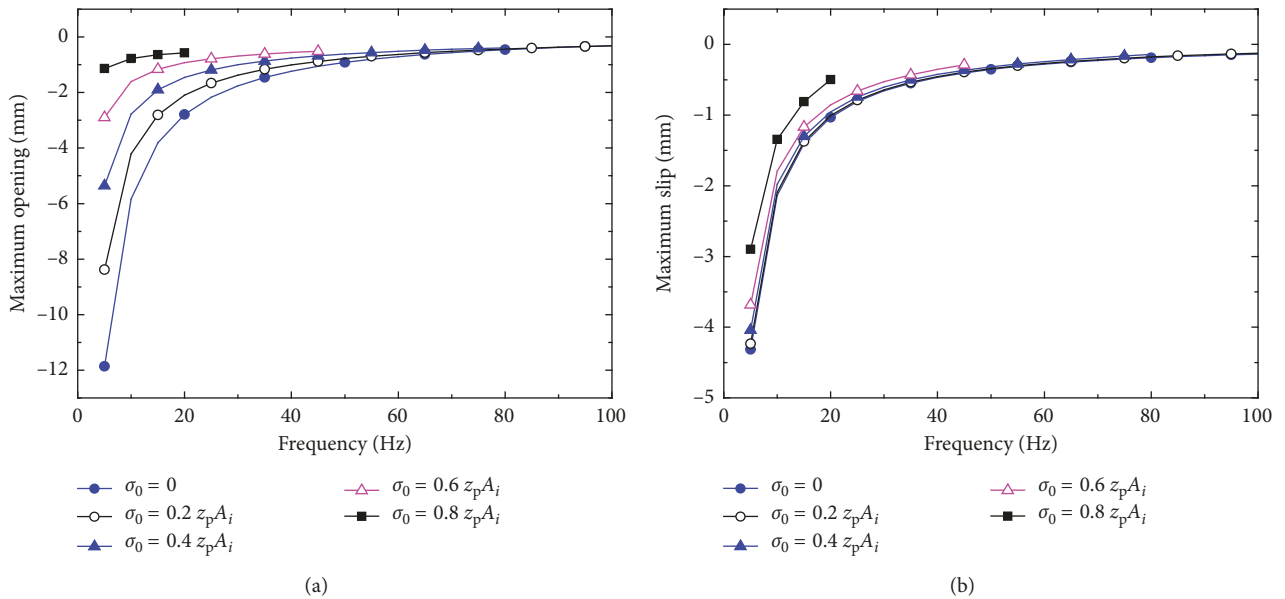


FIGURE 9: Effect of frequency of incidence on the maximum relative deformation of the joint. (a) Maximum opening of a joint ($\alpha = 20^\circ$, incident P-wave). (b) Maximum relative slip of a joint ($\alpha = 20^\circ$, incident P-wave).

smallest. In Figure 9(b), the differences between the maximum slips for σ_0 equal to 0 , $0.2z_p A_i$, and $0.4z_p A_i$ are not obvious. It also can be observed that the joint is not open during wave propagation when the frequency and the in situ stress are higher, such as $f_0 > 20$ Hz and $\sigma_0 = 0.8z_p A_i$. Defining the critical frequency as the value above which the joint is not open, the critical frequency is around 20 Hz for $\sigma_0 = 0.8z_p A_i$, 45 Hz for $\sigma_0 = 0.6z_p A_i$, 80 Hz for $\sigma_0 = 0.4z_p A_i$, and 120 Hz for $\sigma_0 = 0.2z_p A_i$. It indicates that the critical frequency decreases with the increasing in situ stress.

4.3. Effect of Incident Angle on the Maximum Deformation of Joints. Figures 10(a) and 10(b) show the relations between the incident angle α with the maximum opening deformation and slip, respectively. It can be observed that the maximum opening deformation decreases monotonously with increasing incident angle, the maximum slip rises firstly then turn to decreases when α changes from zero to 90° . For a given incident angle, the maximum opening deformation and slip become smaller when the in situ stress is bigger. Defining the critical angle as the value above which no opening mode appears, the critical angle is around 30° for $\sigma_0 =$

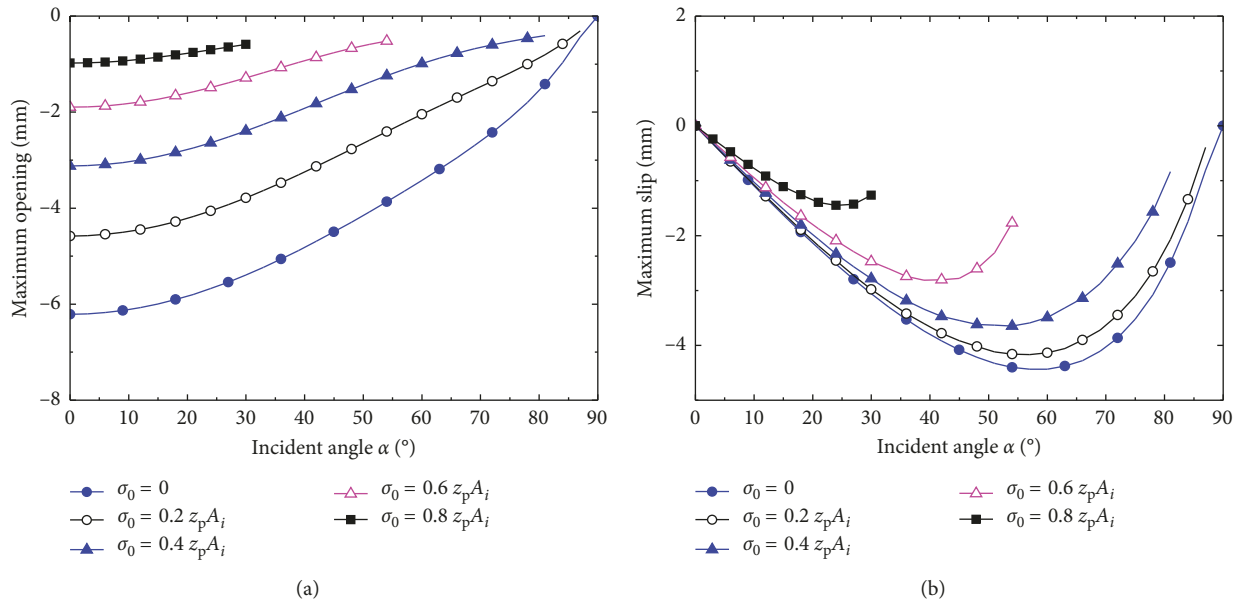


FIGURE 10: Effect of incident angle on the maximum relative deformation of the joint. (a) Maximum opening of a joint ($f = 10$ Hz, incident P-wave). (b) Maximum relative slip of a joint ($f = 10$ Hz, incident P-wave).

$0.8 z_p A_i$, 54° for $\sigma_0 = 0.6 z_p A_i$, 81° for $\sigma_0 = 0.4 z_p A_i$, and 87° for $\sigma_0 = 0.2 z_p A_i$. It can be concluded that the critical angle decreases with the increasing in situ stress.

5. Conclusions

The seismic response for wave propagation with an arbitrary incident angle impinging on joints is analyzed in this paper. Both reflection and transmission usually occurring at the two interfaces of the joint with equally and unequally close-open behaviours are considered. Wave propagation equations of two possible deformation modes, which are close mode and open mode, are deduced, respectively. During the closing process, the joint is assumed to have the normal property with the BB model and the tangential property with linearly elastic. However, once the joint is open, the two interfaces of the joint have no interaction with each other.

Wave propagation across joints with normal and oblique incident P- and S-waves with equally and unequally close-open behaviours is studied and verified by comparing with the existing methods. For the normal case, in situ stress results in the increasing peak values of the transmitted wave, and the cut-off value of the transmitted wave is related to the in situ stress. For the oblique case, compressive portions of the transmitted P-waves are identical, while the tensile portions of the transmitted P-waves are cut off when the particle velocity is less than $-\sigma_0/z_p$. The lower in situ stress easily causes joint open and the slippery deformation of the joint.

The parametric studies on effect of in situ stress on transmitted waves show that the duration of the relative slip decreases with the increasing in situ stress and the particle velocity of the joint caused by the transmitted S-wave increases with increasing in situ stress. When the in situ stress

is smaller, the dominant frequency of the transmitted P-wave is lower. The parametric studies of the effect of incident frequency on the maximum deformation of joints and the effect of incident angle on the maximum deformation of joints are also conducted. Both the maximum opening deformation and the maximum slip of the joint monotonously decrease with increasing incident frequency. The maximum opening deformation decreases with increasing incident angle, and the maximum slip rises firstly and then decreases when incident angle varies from zero to 90° .

Data Availability

All the data used to support the findings of this study are available from the corresponding author upon request.

Conflicts of Interest

The authors declare that there are no conflicts of interest regarding the publication of this paper.

Acknowledgments

This study is supported partially by Natural Science Foundation of Jiangsu Province (BK20150618), Open Research Foundation of the State Key Laboratory for GeoMechanics and Deep Underground Engineering, China University of Mining and Technology (SKLGDUEK1503), the Priority Academic Program Development of Jiangsu Higher Education Institutions (CE01-3-7), Beijing Natural Science Foundation (2184108), China Postdoctoral Science Foundation (2017M620620), and Fundamental Research Funds for the Central Universities (FRF-TP-16-073A1).

References

- [1] N. Barton, "Rock mechanics review, the shear strength of rock and rock joints," *International Journal of Rock Mechanics & Mining Sciences & Geomechanics Abstracts*, vol. 13, no. 9, pp. 255–279, 1976.
- [2] S. R. Brown and C. H. Scholz, "Closure of rock joints," *Journal of Geophysical Research: Solid Earth*, vol. 91, no. B5, pp. 4939–4948, 1986.
- [3] A. Daehnke and H. P. Rossmanith, "Reflection and refraction of plane stress waves at interfaces modeling various rock joints," *Fragblast*, vol. 1, no. 2, pp. 111–231, 1997.
- [4] S. C. Bandis, A. C. Lumsden, and N. R. Barton, "Fundamentals of rock joint deformation," *International Journal of Rock Mechanics & Mining Sciences & Geomechanics Abstracts*, vol. 20, no. 6, pp. 249–268, 1983.
- [5] R. K. Miller, "An approximate method of analysis of the transmission of elastic waves through a frictional boundary," *Journal of Applied Mechanics: Transactions of the ASME*, vol. 44, no. 4, pp. 652–656, 1977.
- [6] M. Schoenberg, "Elastic wave behavior across linear slip interfaces," *Journal of the Acoustical Society of America*, vol. 68, no. 5, pp. 1516–1521, 1980.
- [7] J. Zhao, X. B. Zhao, and J. G. Cai, "A further study of P-wave attenuation across parallel fractures with linear deformational behavior," *International Journal of Rock Mechanics & Mining Sciences*, vol. 43, no. 5, pp. 776–788, 2006.
- [8] X. B. Zhao, J. Zhao, and J. G. Cai, "P-wave transmission across fractures with nonlinear deformational behavior," *International Journal for Numerical & Analytical Methods in Geomechanics*, vol. 30, no. 11, pp. 1097–1112, 2006.
- [9] J. B. Zhu, A. Perino, G. F. Zhao et al., "Seismic response of a single and a set of filled joints of viscoelastic deformational behavior," *Geophysical Journal International*, vol. 186, no. 3, pp. 1315–1330, 2011.
- [10] J. C. Li, H. B. Li, G. W. Ma, and J. Zhao, "A time-domain recursive method to analyze transient wave propagation across rock joints," *Geophysical Journal International*, vol. 188, no. 2, pp. 631–644, 2012.
- [11] J. C. Li, "Wave propagation across non-linear rock joints based on time-domain recursive method," *Geophysical Journal International*, vol. 193, no. 2, pp. 970–985, 2013.
- [12] J. C. Li, X. B. Zhao, H. B. Li, S. B. Chai, and Q. H. Zhao, "Analytical study for stress wave interaction with rock joints having unequally close-open behavior," *Rock Mechanics and Rock Engineering*, vol. 49, no. 8, pp. 3155–3164, 2016.
- [13] H. Kolsky, *Stress Waves in Solids*, Clarendon Press, Oxford, UK, 1953.
- [14] W. Johnson, *Impact Strength of Materials*, Edward Arnold Publishers, London, UK, 1972.
- [15] L. J. Pyrak-Nolte, L. R. Myer, and N. G. W. Cook, "Anisotropy in seismic velocities and amplitudes from multiple parallel fractures," *Journal of Geophysical Research: Solid Earth*, vol. 95, no. B7, pp. 11345–11358, 1990.
- [16] N. G. W. Cook, "Natural joints in rock: mechanical, hydraulic and seismic behaviour and properties under normal stress," *International Journal of Rock Mechanics and Mining Sciences & Geomechanics Abstracts*, vol. 29, no. 3, pp. 198–223, 1992.
- [17] B. L. Gu, R. Sua´rez-Rivera, K. T. Nihei, and L. R. Myer, "Incidence of plane waves upon a fracture," *Journal of Geophysical Research: Solid Earth*, vol. 101, no. B11, pp. 25337–25346, 1996.
- [18] J. C. Li, G. W. Ma, and X. Huang, "Analysis of wave propagation through a filled rock joint," *Rock Mechanics & Rock Engineering*, vol. 43, no. 6, pp. 789–798, 2010.
- [19] J. C. Li and G. W. Ma, "Analysis of blast wave interaction with a rock joint," *Rock Mechanics & Rock Engineering*, vol. 43, no. 6, pp. 777–787, 2010.
- [20] J. Zhao and J. G. Cai, "Transmission of elastic P-waves across single fractures with a nonlinear normal deformational behavior," *Rock Mechanics & Rock Engineering*, vol. 34, no. 1, pp. 3–22, 2001.



Hindawi

Submit your manuscripts at
www.hindawi.com

